Applied Catalysis B: Environmental 86 (2009) 159–165

Contents lists available at ScienceDirect

Applied Catalysis B: Environmental

journal homepage: www.elsevier.com/locate/apcatb

Photocatalytic oxidation of toluene at indoor air levels (ppbv): Towards a better assessment of conversion, reaction intermediates and mineralization

Mohamad Sleiman *, Pierre Conchon, Corinne Ferronato, Jean-Marc Chovelon

Université Lyon 1, CNRS, UMR 5256, IRCELYON, Institut de recherches sur la catalyse et l'environnement de Lyon, 2 avenue Albert Einstein, F-69626 Villeurbanne, France

ARTICLE INFO

Article history:
Received 2 June 2008
Received in revised form 31 July 2008
Accepted 3 August 2008
Available online 9 August 2008

Keywords:
Photocatalysis
VOC
Toluene
Indoor air
Reaction products

ABSTRACT

We report here a new analytical methodology for the investigation of toluene photocatalytic removal at indoor-relevant concentration level (ppbv). Experiments were performed using an annular flow-through reactor with TiO_2 as photocatalyst, toluene as a model VOC and under different ranges of relative humidity (RH: 0–70%), inlet concentration (20–400 ppbv) and flow rate (70–350 mL min^{-1}). Analysis of reaction intermediates was conducted using an automated thermal desorption technique coupled to GC–MS instrument (ATD–GC–MS) whereas a GC coupled to pulsed discharge helium ionization detector (GC–PDPID) was used for the first time for on-line measurements of CO and CO_2 at ppbv level.

Under these conditions, toluene conversion was up to 90–100% with a slight influence of inlet concentration and RH, whereas flow rate was found to be a prevalent factor. Mineralization (%) varied from 55 to 95% and has shown to be strongly inhibited by the increase of RH whereas flow rate and inlet concentration exhibited a negligible effect. The reaction intermediates were found to be different according to the RH level: in absence of water vapor, traces of low molecular weight carbonyls (formaldehyde, methyl glyoxal, etc.) were detected and quantified in the gas phase whereas at RH 40%, hydroxylated intermediates such as cresols and benzyl alcohol were observed. On the basis of identification results, a reaction mechanism was proposed involving mainly direct hole oxidation at dry conditions and hydroxylation by OH radicals at high RH level.

1. Introduction

Recently, with the increasing concerns on indoor air quality (IAQ) [1], photocatalytic oxidation (PCO) has received growing interests as a promising technology for the removal of indoor air pollutants, in particular volatile organic compounds (VOCs) present at low ppb concentrations [2,3]. Unlike conventional air cleaning technologies such as filtration and sorption [4], which only transfer indoor pollutants to another phase, this method has the potential to destroy a broad range of VOCs to carbon dioxide (CO_2) and water (H_2O) [5,6]. Furthermore, PCO is a cost-effective method because it operates at room temperature and the photocatalyst (TiO_2) is inexpensive and widely available.

In the past few years, several studies have been made to assess the feasibility of PCO for the removal of VOCs at typical indoor concentration levels (ppbv range) [7–12]. Moreover, the influence of several practical parameters such as VOC concentration, relative humidity, UV light intensity, mass transfer, etc., on VOC removal efficiency was investigated [10,13–17]. Nevertheless, there are still some relevant unanswered issues which represent challenges for a better comprehension of the PCO process and its commercialization for indoor air applications [18]. For example, in many studies a little attention has been paid to the analysis of reaction intermediates which can be in some cases more toxic and/or stable than the parent VOC [10,19]. Furthermore, no information is available so far on the VOC mineralization (CO_2 yield) at low ppbv concentrations and its dependence on the different operational parameters. On the other hand, the role of water in the reaction process is yet unclear, though a large number of studies was devoted to this aspect [15,16,20,21].

The present work addresses these problems and presents an experimental approach using advanced analytical methods (ATD–GC–MS and GC–PDPID) to undertake a systematic study of toluene PCO, at typical indoor air levels (20–400 ppbv). Toluene was chosen as a model VOC, because it belongs to BTEX, a major group frequently encountered in indoor air in different countries [1]. Moreover, toluene has been classified as one of eight representative indoor VOCs by a proposed ASHRAE (American Society of

* Corresponding author. Tel.: +33 4 72 43 11 50; fax: +33 4 72 44 84 38.
E-mail address: mohamad.sleiman@ircelyon.univ-lyon1.fr (M. Sleiman).

0926-3373/$ – see front matter © 2008 Elsevier B.V. All rights reserved.
doi:10.1016/j.apcatb.2008.08.003

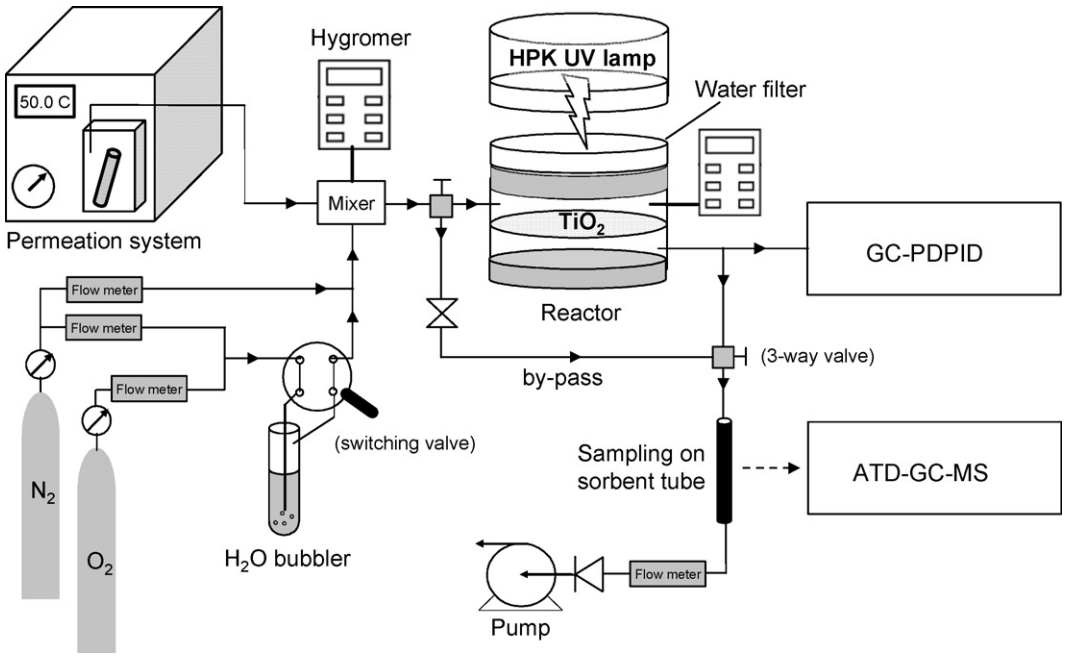

Fig. 1. Schematic representation of the experimental set-up used for the PCO of toluene.

Heating, Refrigerating, and Air-Conditioning Engineers) test method for determining the efficiency and capacity of gas-phase air cleaning systems for indoor air applications [22].

2. Experimental

2.1. Reactor and experimental set-up

Fig. 1 shows a schematic representation of the experimental set-up used for the PCO of toluene in gas phase. Experiments were conducted in continuous flow mode using an annular flow-through reactor of about 85 mL, made of stainless steel and equipped with an optical Pyrex glass window (transmittance: wavelength >290 nm), a water cell to avoid heating and a high pressure mercury UV lamp (HPK 125 W, Philips). The photocatalytic medium was a non-woven fibrous paper, coated with TiO_2 PC500 (100% anatase, BET area: 300 $m^2\,g^{-1}$, crystal size: 5–10 nm) supplied by Ahlstrom, France.

A gaseous stream of toluene was generated using a permeation tube from Calibrage (France) filled by pure liquid toluene and placed inside a furnace maintained at a constant temperature of 50 °C. A N_2 gas at a constant flow rate of 50 mL min^{-1} was passed over the permeation tube and subsequently mixed with O_2, N_2 or He and water vapor (H_2O) at gas flow rates corresponding to target toluene concentration ranging from 20 to 400 ppbv. The gas flow rates were adjusted using mass flow controllers in the 0–200 mL min^{-1} range (Brooks, 5850S series). The final gas stream humidity and temperature were measured using a thermohygrometer (Rotonic Hygropalm 1, France). Prior to all photocatalytic experiments, the photocatalyst medium was pretreated by UV irradiation in an oxygen/N_2 (20/80 v:v) gas flow for 12–24 h to insure an efficient elimination of adsorbed contaminants on the surface. The standard operating conditions used for irradiation experiments are summarized in Table 1.

2.2. Sampling and analysis of gaseous intermediates

During the irradiation experiments, toluene and gas phase reaction intermediates were collected for 5–30 min at regular time intervals and at flow rate of 30 mL min^{-1} using multibed solid sorbent tubes packed with Carbotrap C, Carbotrap B and Carbosieve SIII (Supelco) in that order. In preliminary experiments, the sampling conditions were tested against breakthrough by collecting a 600 mL sample of toluene and several standards of potential degradation intermediates (benzene, phenol, benzaldehyde, benzyl alcohol) with two identical tubes connected in series. The analysis showed no breakthrough from the first trap to the second one, confirming that no lost of products occurs during the sampling step (5 min, 150 mL). On the other hand, the repeatability of the whole analytical procedure (sampling and analysis) was measured with a series of 6 samples of standards and the resulting relative standard deviation was <2%. Analysis was carried out using a GC–MS (Clarus 500, PerkinElmer,) equipped with an automated thermal desorption unit (Turbomatrix, PerkinElmer). MS identification was conducted (i) by comparing the retention times and mass spectra to available authentic standards, (ii) by using the NIST library with a fit higher than 90%. An effort was also made to quantify the major reaction intermediates present in gas phase in order to determine the main reaction routes and to better understand the reaction mechanisms. All analytes were quantified using ATD–GC–MS multipoint calibration curves developed from pure chemical standards, purchased from Aldrich.

For analysis of formaldehyde and low molecular weight carbonyls potentially formed in gas phase, air samples at outlet of the reactor were collected onto sampling tubes packed with Tenax (50 mg) that was precoated with 300 nmol of the

Table 1
Experimental conditions for the PCO of toluene

Experimental parameter	Value
Inlet toluene conc. (ppbv)	20–400
Relative humidity (%)	0–70
Flow rate (mL min^{-1})	70–350
Reaction temperature (K)	298 ± 2
TiO_2 area density (g m^{-2})	5
UV intensity (mW cm^{-2})	4.3
Oxygen (% in He)	2
Catalyst surface (cm^2)	16

Table 2
ATD–GC–MS operating parameters

Step	Parameter	Value
Tube desorption	Focusing trap temp.	−30 °C
	Desorption temp.	280 °C
	Desorption time	10 min
Trap desorption	Desorption temp.	325 °C
	Desorption time	5 min
	Split ratio	10
	Transfer line temp.	200 °C
GC separation	Carrier gas	He (1.7 mL min^{-1})
	Capillary column	Elite 5-MS (60 m × 0.25 mm × 1 μm)
	Oven temperature program	50 °C (2 min), 10 °C min^{-1} to 270 °C (6 min)
MS detection	Source temp.	200 °C
	Electron energy	70 eV
	Scan range (*m*/*z*)	33–500

derivatization agent PFPH (pentafluoro phenylhydrazine, 97% purity purchased from Aldrich). The flow rate was 30 mL min^{-1} and sampling duration varied from 15 min to 2 h. Coating was achieved by injecting a known amount of PFPH into the Tenax sampling tube using the injector of a gas chromatograph, heated at 220 °C. After collection, tubes were stored for 3 h at ambient temperature before analysis by means of ATD–GC–MS technique (analytical conditions identical to those reported in Table 2). Using this procedure, detection limits (LOD) for formaldehyde and acetone were less than 0.05 and 0.1 ppbv, respectively, which are much better than those usually obtained by the DNPH-HPLC method.

2.3. On-line measurements of CO/CO_2

The formation of CO/CO_2 during the reaction was monitored every 1 h using a GC–PDPID instrument [23,24] that consisted of: (i) one 10-way Valco valve (V10) equipped with a 1 mL sample loop, (ii) two packed chromatographic columns placed in parallel configuration: a Porapack Q (L: 5 m, ID: 1/8″) and a Tamis 13-X (L: 2 m, ID: 1/16″) from RESTEK, (iii) a D4-I detector (Valco instruments). The carrier gas was ultra pure He N60 from Air Liquide which was additionally purified by a Valco HP-2 purifier. Oven temperature was 40 °C and column flow rates were 8 mL min^{-1} for Tamis 13-X and 25 mL min^{-1} for Porapack Q. Using these conditions, analysis time was around 5 min. Calibration of CO/CO_2 was carried out using a standard mixture of CO/CO_2 (5 ppmv in He). The detection limits for CO and CO_2 were 40 and 20 ppbv respectively, with a relative standard deviation of 0.8% for CO and 0.2% for CO_2. It should be pointed out that He was used instead of N_2 and only 2% Oxygen in He was employed during all irradiation experiments in order to avoid the overlapping of chromatographic peaks of N_2/ O_2 with those of CO/CO_2 during the GC–PDPID analysis.

2.4. Analysis of adsorbed species

Adsorbed species on the TiO_2 surface were identified using two procedures: the first one consists on a solid–liquid extraction using a solvent mixture of methanol/water (20/80 v/v)) adjusted at pH 8 with NaOH, followed by ion chromatography, HPLC–UV and GC–MS analyses. The second procedure was a controlled thermal desorption of the photocatalyst medium, followed by GC–MS analysis.

3. Results and discussion

A series of experiments was conducted to evaluate the effect of three important parameters (inlet concentration, flow rate and relative humidity) on the single-pass conversion and mineralization efficiencies of toluene. Experiments were carried out in triplicate and data were collected under steady state (30 min to 1 h are required for the experimental system to reach a steady state after the experiment started). It is worthy to note that in preliminary experiments, the effect of oxygen content in the range 2–20%, on the photocatalytic activity (conversion of toluene) was found to be negligible.

The conversion of toluene was calculated from the difference between the inlet and outlet toluene concentrations, as:

$$\%\,\text{Conversion} = \frac{[\text{Toluene}]_{\text{in}} - [\text{Toluene}]_{\text{out}}}{[\text{Toluene}]_{\text{in}}} \times 100$$

Whereas the mineralization extent (%) was determined by comparing the concentration of carbon dioxide (CO_2) produced to the theoretical one (if mineralization is complete: 1 mole of toluene should lead to the formation of 7 moles of CO_2), using the following equation:

$$\%\,\text{Mineralization} = \frac{[CO_2]_{\text{measured}}}{[CO_2]_{\text{theoretical}}} \times 100$$

where

$$[CO_2]_{\text{theoretical}} = \frac{7 \times \%\,\text{conversion} \times [\text{Toluene}]_{\text{in}}}{100}$$

3.1. Effect of flow rate

Fig. 2 shows the variation of both conversion and mineralization of toluene as a function of flow rate in the range 70–350 mL min^{-1} (corresponds to residence time: 0.8–4 min). Experiments were conducted with toluene inlet concentration of 120 ppbv at RH of 40% and UV intensity of 4.3 mW cm^{-2}.

As it can be seen, an increase of flow rate results in a significant decrease of toluene conversion (from 95 to 65%). A similar behavior was observed by Jeong et al. [25] for the degradation of toluene at low concentrations. In general, when the flow rate increases, two antagonistic effects are brought into play: the decrease in residence time within the photocatalytic reactor and the increase in the mass transfer rate [14]. In our conditions, the diminution of conversion with the flow rate implies that contact time between

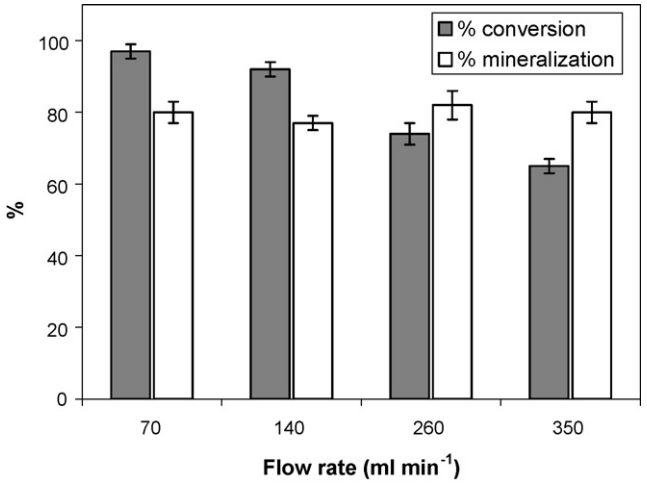

Fig. 2. Influence of flow rate on the conversion (%) and mineralization (%) of toluene (inlet concentration: 120 ppbv, RH: 40%).

toluene molecules and TiO_2 surface is the prevalent factor. It should be pointed out that this phenomenon seems to be related to the nature of reactant and probably to its affinity with the surface. For example, in our previous study [26] and using the same experimental conditions, the conversion of dichlorvos (organophosphorus pesticide) was found to be unaffected by the variation of flow rate. This difference could be attributed to the fact that dichlorvos is much more strongly adsorbed on the TiO_2 surface and thereby, the contact time effect becomes less important. Further studies on multiple compounds with different chemical structures, should confirm or deny this hypothesis.

On the other hand, the mineralization of toluene seems to be independent on the flow rate. This means that residence times in the studied range (0.8–4 min) are sufficient to achieve the series of PCO reactions leading to CO_2. Although this behavior appears to be surprising since conversion was decreased by the increase of flow rate, conversion of toluene corresponds only to the initial step of the degradation process and it depends strongly on the transfer of toluene from gas phase to the surface. In contrary, mineralization is the result of multiple surface PCO reactions of intermediates leading to CO_2, where flow rate exhibits very limited influence, in particular if intermediates are not displaced from the surface to the gas phase.

3.2. Effect of inlet concentration

Langmuir–Hinshelwood (L–H) rate expression has been widely used [16,27] to describe the gas–solid phase reaction for heterogeneous photocatalysis. Assuming that the mass transfer is not the limiting step and that the effect of intermediate product is negligible, then the reaction rate in a plug-flow reactor can be expressed as:

$$r = -u\frac{dC_{toluene}}{dL} = \frac{kKC}{1+KC} \quad (1)$$

where k and K are the L–H reaction rate constant and the L–H adsorption equilibrium constant, L is the length of the photoreactor and u is the gas velocity through the reactor. After rearrangement and integration of Eq. (1) the following linear expression can be obtained [9]:

$$\frac{\ln(C_{in}/C_{out})}{(C_{in}-C_{out})} = \frac{kK(V/F)}{(C_{in}-C_{out})} - K \quad (2)$$

where C_{in} and C_{out} are the inlet and outlet concentrations of toluene, respectively, υ is the volume of the reactor (85 mL), F is the flow rate through the reactor (150 mL min^{-1}).

If L–H model is valid, a plot of $\ln(C_{in}/C_{out})/(C_{in}-C_{out})$ versus $1/(C_{in}-C_{out})$ should be linear. As shown in Fig. 3, the experimental data are in good agreement with the integral rate law analysis and a linear relationship is observed (R^2 = 0.999). The obtained values of k and K are 213 ppb min^{-1} and 0.0025 ppb^{-1}, respectively. This finding suggests that reaction occurs on the photocatalyst surface through a L–H mechanism and not in the gas phase.

On the other hand, the inset in Fig. 3 displays the dependence of both conversion and mineralization (%) on the toluene inlet concentration. We note that inlet concentration does not exert any significant influence on both parameters. This indicates that at this range of toluene concentration, the PCO is not limited by the number of active sites on TiO_2 and no competitive adsorption effect between the byproducts and toluene occurs. In contrary, at high ppmv range of concentration the phenomenon of catalyst saturation and adsorption competition is usually observed [28]. This is one of the reasons why photocatalysis is well suited for the degradation of gaseous effluents at ppbv concentration levels.

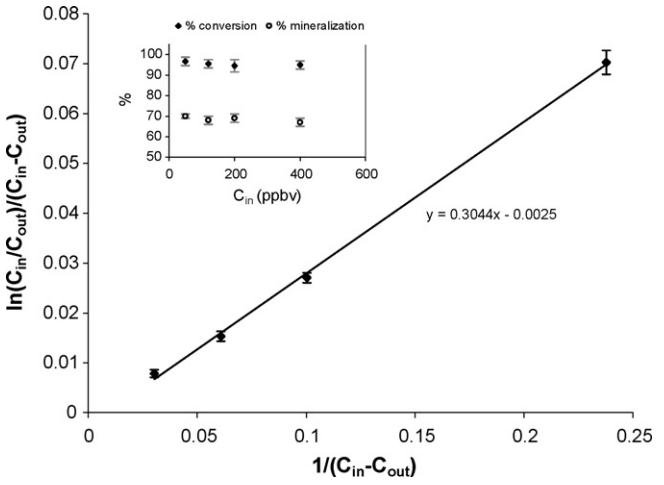

Fig. 3. Plot of $\ln(C_{in}/C_{out})/(C_{in}-C_{out})$ vs $1/(C_{in}-C_{out})$ according to L–H rate expression. Data were obtained under gas flow rate of 150 mL min^{-1} and RH 40% (the inset shows the effect of inlet concentration on the conversion % and mineralization % of toluene).

3.3. Effect of relative humidity

The effect of relative humidity on the PCO efficiency (conversion and mineralization) was tested using different RH levels ranging from 0 to 70% (water vapor concentration from 1 to 20,000 ppmv) and a fixed concentration of toluene of 120 ppbv. Results are illustrated in Fig. 4.

We note that the behaviors of conversion and mineralization as a function of RH are widely different. The conversion appears to be independent on the RH in the range 0–20% whereas at higher water concentrations (>6000 ppmv), it decreases slightly from 95 to 85%. The conversion decline at high RH level is likely due to a competition of adsorption between water molecules and toluene, as already reported by several authors [9,13,16]. Zhang et al. [21] suggested that water molecules can physisorb on the surface hydroxyl groups via hydrogen bonding and form at relatively moderate RH (15–25%) a film composed of one or several layers which prevents or retards the pollutant from reaching the reactive TiO_2 surface or contacting radical species in the boundary layer.

On the other hand, no optimum humidity level was found at low RH, which seems to be inconsistent with the results of Obee [16] who showed that for a low toluene concentration (290 ppbv), reaction rate increases at low RH level to reach a maximum located

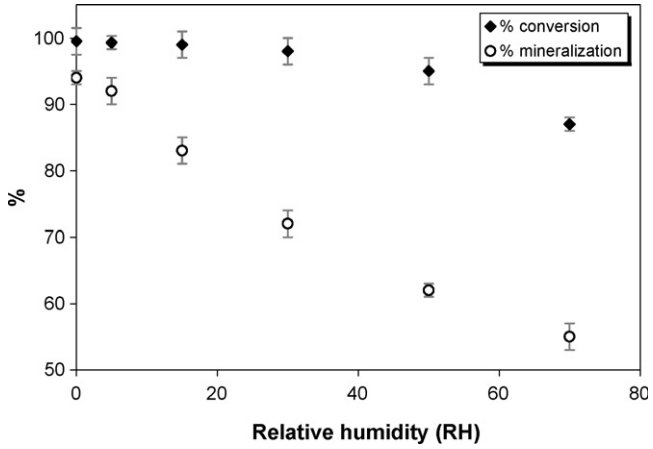

Fig. 4. Effect of relative humidity on the conversion and mineralization of toluene (inlet conc.120 ppbv, flow rate: 150 ml min^{-1}).

around 5% RH. The authors have explained this rate increase by an increase in population of $OH^{\bullet}$ radicals, which were supposed to be the primary oxidant during PCO.

The discrepancy between our study and the results found by Obee [16] may arise from the use of different inlet toluene concentrations (120 ppbv versus 290 ppbv in [16]) since authors showed that the location of maximum conversion shifts significantly to lower humidity levels as toluene concentration is decreased. This means that in our conditions (toluene conc. 120 ppbv), an optimum humidity level could be present at very low RH (near 0% RH). Nevertheless, it could not be clearly detected due to the very high toluene conversion and the moderate accuracy of RH measurement by the hygromer (1%). This reflection is corroborated by the results of Ao et al. [13] and Jo et al. [15], who also did not observe any optimum humidity level for the conversion trends of BTEX at concentrations ranging from 10 to 50 ppbv.

Even though this speculation can be valid to explain the absence of a "visible" optimum humidity level, it cannot justify the observed quasi-total conversion and mineralization of toluene in the absence of water vapor in gas phase (0% RH). D'Hennezel et al. [29] showed that holes (h^+) mediated toluene oxidation is more important reaction pathway than oxidation by $OH^{\bullet}$. Thus, we suggest that the observed limited influence of RH on the toluene conversion is related to the fact that $OH^{\bullet}$ radicals are not the main active species during the PCO of toluene. This implies that the effect of relative humidity on pollutant conversion is not governed only by its concentration but also by the reaction mechanisms. Looking at the evolution profile of mineralization as function of RH level, we can see clearly that it is considerably reduced by the increase of RH. Two probable reasons can be invoked to explain this behavior. The first one is the adsorption competition between water molecules and weakly adsorbed intermediates which can be desorbed from the surface to gas phase without being degraded [30]. The second one is that reaction intermediates are different according to the RH level and that at high RH level some strongly bound surface species are formed and are slowly mineralized into CO_2 [31].

To check out the validity of these assumptions, a careful analysis of reaction intermediates and a study of the relationship of their distributions with the RH were performed. The results are discussed below in the next paragraph.

3.4. Reaction products

Although several studies have investigated the gas-phase PCO of toluene at ppbv level [8,13,16,32], they have focused on the PCO rates rather than on the identification of reaction intermediates. In this work, a special attention was devoted to the analysis of reaction products and their quantification at different RH in order to evaluate the feasibility of such treatment for indoor air applications but also to understand the role of water and get insight into the reaction mechanisms.

3.4.1. Reaction products in gas phase

Table 3 summarizes the different intermediates detected in gas phase and their concentrations during the degradation of toluene (120 ppbv) under two RH levels: 0 and 40%.

In all experiments, we note that: benzaldehyde was the main gaseous intermediate, which is consistent with the results reported by several authors on the toluene PCO at high ppmv concentrations [33–35]. Benzene seems to be also a common product under both RH levels, but it is present at very low concentrations. No CO production was detected under all RH level. Since the detection limit of GC–PDPID for CO is around 40 ppbv, this result does not imply absolutely that CO was not produced during the PCO of toluene. Einaga et al. [35] reported the formation of a small amount of CO during the PCO of high toluene concentrations (>100 ppmv). To check out the production of CO, a PCO experiment was conducted with 800 ppbv of toluene. Results revealed no traces of CO under both dry and humid conditions which indicates that at low ppbv concentration the PCO oxidation has a much better selectivity to CO_2 than that found at higher concentrations.

Table 3
MS data and concentrations of PCO gaseous products of toluene (120 ppbv), at 0 and 40% RH

Product	MS data (fragment, m/z)	Concentration (ppbv)	
		0% RH	40% RH
Toluene	92, 91, 65	5.8	7.5
Benzaldehyde	106, 105, 77	3.2	4.1
Benzene	78, 77, 51	0.9	1.3
Benzyl alcohol	108, 107, 79, 77	–	0.9
Phenol	94, 66, 65	–	0.7
(*o*, *m*-*p*)-cresol	108, 107	–	2.0
Formaldehyde-PFPH	210, 182, 155	1.4	0.6
Methyl glyoxal	432, 250, 182, 155	1.1	–
Vinyl methyl ketone	250, 182, 155	0.8	–
CO	–	–	–
CO_2	–	790	550

It is interesting to note that traces of formaldehyde, methyl vinyl ketone and methyl glyoxal were found at dry conditions whereas at humid conditions, only traces of formaldehyde were detected in gas phase. This difference could be related to the formation at high RH level of ultra-hydrophilic layers leading to the promotion of adsorption of aldehyde/acid intermediates. To the best of our knowledge, this is the first time that such small carbonyls are detected during the PCO of toluene. Most likely, these molecules resulted from the aromatic ring opening as reported by Irokawa et al. [36] who observed the formation of wide variety of carboxylic acids (oxalic, acetic and formic, etc.) and aldehydes (formaldehyde, acetaldehyde) through ring cleavage processes during toluene photoxidation over $TiO_{2-x}N_x$ under visible light irradiation.

In contrast, at humid conditions exclusively, several hydroxylated products such as cresols, phenol, and benzyl alcohol were produced. Nevertheless, the overall concentration of intermediates in gas phase has not been considerably increased at humid conditions and no significant desorption of benzaldehyde, or benzene occurred. Thus, the hypothesis that adsorption competition with water molecules leads to a partial desorption of intermediates from the surface, as discussed earlier, is not plausible to explain the drop of toluene mineralization yield observed with the increase of RH.

3.4.2. Reaction products adsorbed on TiO_2

The analysis of adsorbed species on TiO_2 surface could be helpful to find out more about the reaction mechanisms and also the impact of relative humidity on the reaction process. Table 4 presents the detected adsorbed species and their relative amounts found at two RH levels (0 and 40%) after 1 and 3 days of toluene PCO. As it can be seen, benzaldehyde, benzoic acid and traces of benzene and formic acid were found at both RH levels. On the contrary, cresols, benzyl alcohol, 3-hydroxybenzaldehyde, hydroquinone were detected only at 40% RH. Furthermore, at 40% RH, hydroxylated intermediates such as cresols, hydroquinone and hydroxybenzaldehyde were found to accumulate on the surface during PCO of toluene. This indicates

Table 4
Adsorbed species on TiO_2 after 1 and 3 days of toluene PCO (44 nmol h^{-1}, 120 ppbv), at 0 and 40% RH

Product	0% RH		40% RH	
	24 h	72 h	24 h	72 h
Benzaldehyde	+	+	+	+
Benzoic acid	+	+	+	+
Benzyl alcohol	–	–	+	+
Formic acid	+	+	+	+
3-Hydroxy benzaldehyde	–	–	+	++[a]
Hydroquinone	–	–	+	++
Cresols	–	–	+	+++

[a] ++ Corresponds to two times the peak area (+) of the intermediate obtained at 0% RH.

that hydroxylated species are relatively slowly degraded and are likely responsible for the drop of toluene mineralization (%) when RH increased. This proposition is consistent with the results of Larson and Falconer [37] who reported that the adsorbed *m*-cresol was hardly oxidized by TiO_2 photocatalysis and the catalyst turned to black due to the polymerization of *m*-cresol to polyphenolic compounds.

At high toluene concentrations, TiO_2 deactivation has been frequently reported in the literature [34,38–40]. Several authors found that photocatalyst change its color from white to yellow or yellow-brown after several hours of irradiation. This was generally attributed to the accumulation of strongly adsorbed species such as benzaldehyde and benzoic acid on TiO_2 surface [36,41–43]. However, in our conditions, data show that no significant accumulation of both species over time appears to occur. The discrepancy between our results and those already observed in previous works [34,38,40] indicates that the inlet pollutant concentration could drastically affects the intermediates accumulation and catalyst deactivation.

On the other hand, in our case, despite the partial accumulation of hydroxylated intermediates, no evidence of loss of photocatalytic activity was observed within 48 h of experiment. The toluene mineralization yield (%) was always identical to that observed in the first hours of irradiation (65%). This can be attributed to the low amounts of accumulated species on the surface, compared to those found by other authors [29,34,38] where concentrations of toluene were at least hundred times higher than those used in our study.

3.5. Reaction pathways

Fig. 5 presents a tentative reaction scheme for the PCO of toluene in gas phase. On the basis of our results and literature data, two competitive reaction pathways appear to occur according to the RH level. The occurrence of two different pathways could be related to the competition of different active species but also to the adsorption mode(s) of toluene on the TiO_2 surface. Previous studies [43,44] have shown using FTIR *in situ* that toluene is adsorbed in a flat orientation with its ring parallel to the catalyst surface through the formation of a $Ti^{4+}\cdots\pi$ electron type complex on the dehydroxylated surface and by the formation of a $OH\cdots\pi$ electron type complex on the hydroxylated surface. These findings let us suppose that RH level could affect the adsorption mode of toluene and induces a change in the mechanisms of initial reaction steps.

3.5.1. Pathway (1)

At low RH or in absence of water vapor, the reaction is mainly initiated via an electron transfer from toluene to TiO_2 with the formation of an aromatic radical cation and a benzyl radical [29]. Benzyl radical can react then with O_2 to form a benzylperoxy radical which decomposes thermally on the surface to give benzaldehyde and hydroxyl radical ($OH^{\bullet}$), as proposed by Coronado and Soria [45]. Meanwhile, the aromatic radical cation can also react with oxygen and form an aromatic bridged peroxo intermediate. This structure is unstable and undergoes a fast opening of the aromatic ring which leads to the release of several aliphatic carbonyls. To our knowledge, this ring opening route has never been proposed in photocatalysis studies. Nevertheless, the fast toluene mineralization observed in our study associated with the evidences found on the formation of carbonyls let us suggest that this route may exist. Further investigations are however necessary to confirm the presence of such pathway.

Benzaldehyde can be further oxidized to benzoic acid which in turn decomposes on the TiO_2 surface via a photoKolbe mechanism giving rise to benzene and CO_2. The reaction proceeds by a series of oxidation steps by holes (h^+), oxygen and $OH^{\bullet}$ radicals at lesser extent, leading finally to the formation of CO_2.

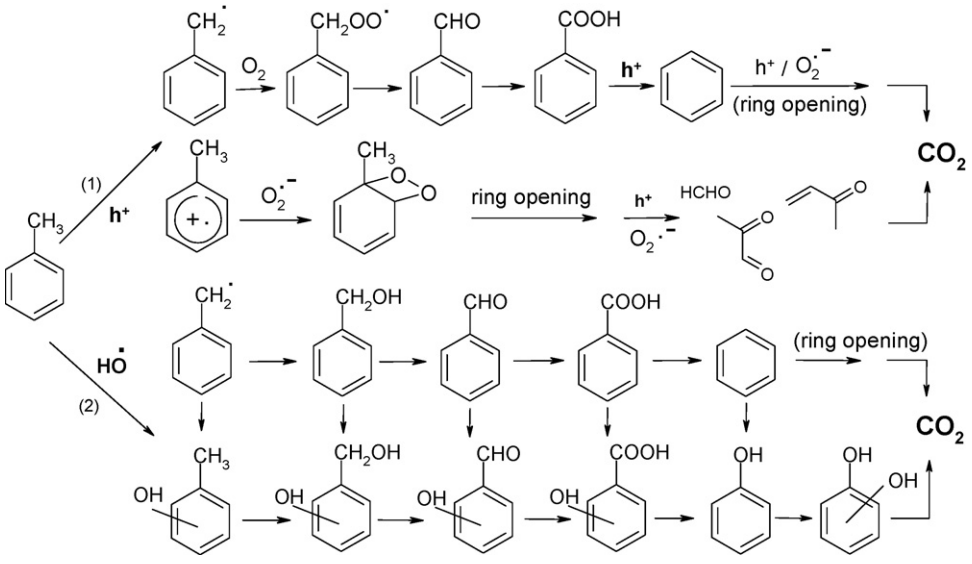

Fig. 5. Proposed reaction pathways for the PCO of toluene in gas phase.

3.5.2. Pathway (2)

This pathway seems to be minor at low RH level, whereas at high RH level it is enhanced by the increase in population of $OH^{\bullet}$ radicals.

The first step in this route is either an addition of $OH^{\bullet}$ radical on the aromatic ring of toluene leading to the formation of cresols (*o*, *m*, *p*-cresol) or the H-abstraction from toluene methyl group by OH radical resulting in the production of benzyl alcohol. The latter can be oxidized to benzaldehyde and later on to benzoic acid, which undergoes a photoKolbe reaction, as discussed above, to give benzene and CO_2. At the same time, a series of hydroxylations of the aromatic ring steps can take place and give rise to several hydroxylated intermediates (hydroxyl benzaldehyde, hydroquinone, etc.) which are slowly mineralized to CO_2.

The proposed reaction scheme here is consistent with the different products identified. However, it is clear that its verification needs further investigation of the evolution of reaction intermediates during the PCO of toluene. Unfortunately, this was not feasible due to the low concentrations of toluene used.

4. Conclusions

In this paper, a novel methodology for the analysis of toluene photocatalytic reaction products (CO_2, organic intermediates) at ppbv level has been presented. This sort of information was missing in previous studies and is relevant for the evaluation of PCO efficiency and its feasibility for indoor air applications.

The results showed that toluene conversion (%) and mineralization (%) exhibited different trends as a function of flow rate and RH level. This implies that it is not possible to conclude on the efficiency of PCO process without taking into account both parameters (conversion and mineralization). The RH level was found to be a key factor in the reaction processes. At low RH, high mineralization extent (~90%) can be achieved but some dangerous products such as small aldehydes are produced in the gas phase. In contrary, at high RH levels, the mineralization rate is slower due to the formation of strongly adsorbed species such as cresols, phenol and acidic intermediates.

Taking into account the results obtained in this study, more systematic works are needed to provide important data on the reaction products and mineralization extent under the concentrations levels typically found in indoor environment.

Acknowledgement

The authors thank Joseph Dussaud (Ahlstrom) for supplying the photocatalytic papers.

References

[1] A.P. Jones, Atmospheric Environment 33 (28) (1999) 4535–4564.
[2] J. Zhao, X. Yang, Building and Environment 38 (5) (2003) 645–654.
[3] S. Wang, H.M. Ang, M.O. Tade, Environment International 33 (5) (2007) 694–705.
[4] D.W. VanOsdell, M. Kathleen Owen, L.B. Jaffe, L.E. Sparks, Journal of the Air and Waste Management Association 46 (9) (1996) 883–890.
[5] J. Peral, X. Domenech, D.F. Ollis, Journal of Chemical Technology and Biotechnology 70 (2) (1997) 117–140.
[6] P. Pichat, J. Disdier, C. Hoang-Van, D. Mas, G. Goutailler, C. Gaysse, Catalysis Today 63 (2–4) (2000) 363–369.
[7] L. Stevens, J.A. Lanning, L.G. Andersen, W.A. Jacoby, N. Chornet, Journal of the Air and Waste Management Association 48 (10) (1998) 979–984.
[8] K. Demeestere, J. Dewulf, B. De Witte, A. Beeldens, H. Van Langenhove, Building and Environment 43 (4) (2008) 406–414.
[9] C.H. Ao, S.C. Lee, J.Z. Yu, J.H. Xu, Applied Catalysis B: Environmental 54 (1) (2004) 41–50.
[10] A.T. Hodgson, H. Destaillats, D.P. Sullivan, W.J. Fisk, Indoor Air 17 (4) (2007) 305–316.
[11] C.H. Ao, S.C. Lee, Applied Catalysis B: Environmental 44 (3) (2003) 191–205.
[12] T. Salthammer, F. Fuhrmann, Environmental Science & Technology 41 (18) (2007) 6573–6578.
[13] C.H. Ao, S.C. Lee, C.L. Mak, L.Y. Chan, Applied Catalysis B: Environmental 42 (2) (2003) 119–129.
[14] P.F. Biard, A. Bouzaza, D. Wolbert, Environmental Science & Technology 41 (8) (2007) 2908–2914.
[15] W.K. Jo, K.H. Park, Chemosphere 57 (7) (2004) 555–565.
[16] T.N. Obee, Environmental Science & Technology 29 (5) (1995) 1223–1231.
[17] I. Salvado-Estivill, D.M. Hargreaves, G. LiPuma, Environmental Science & Technology 41 (6) (2007) 2028–2035.
[18] D.T. Tompkins, B.J. Lawnicki, W.A. Zeltner, M.A. Anderson, ASHRAE Transactions, 2005.
[19] A. Wisthaler, P. Strøm-Tejsen, L. Fang, T.J. Arnaud, A. Hansel, T.D. Mark, D.P. Wyon, Environmental Science & Technology 41 (1) (2007) 229–234.
[20] C. Raillard, V. Hequet, P. Le Cloirec, J. Legrand, Journal of Photochemistry and Photobiology A: Chemistry 163 (3) (2004) 425–431.
[21] L. Zhang, W.A. Anderson, S. Sawell, C. Moralejo, Chemosphere 68 (3) (2007) 546–553.
[22] W. Chen, J.S. Zhang, Z. Zhang, ASHRAE Transactions, 2005.
[23] D.S. Forsyth, Journal of Chromatography A 1050 (1) (2004) 63–68.
[24] W.E. Wentworth, K. Sun, D. Zhang, J. Madabushi, S.D. Stearns, Journal of Chromatography A 872 (1–2) (2000) 119–140.
[25] J. Jeong, K. Sekiguchi, W. Lee, K. Sakamoto, Journal of Photochemistry and Photobiology A: Chemistry 169 (3) (2005) 279–287.
[26] M. Sleiman, C. Ferronato, J.M. Chovelon, Environmental Science & Technology 42 (8) (2008) 3018–3024.
[27] S.B. Kim, S.C. Hong, Applied Catalysis B: Environmental 35 (4) (2002) 305–315.
[28] A. Bouzaza, C. Vallet, A. Laplanche, Journal of Photochemistry and Photobiology A: Chemistry 177 (2–3) (2006) 212–217.
[29] O. D'Hennezel, P. Pichat, D.F. Ollis, Journal of Photochemistry and Photobiology A: Chemistry 118 (3) (1998) 197–204.
[30] A.J. Maira, J.M. Coronado, V. Augugliaro, K.L. Yeung, J.C. Conesa, J. Soria, Journal of Catalysis 202 (2) (2001) 413–420.
[31] K. Demeestere, J. Dewulf, B. De Witte, H. van Langenhove, Applied Catalysis B: Environmental 60 (1–2) (2005) 93–106.
[32] A. Strini, S. Cassese, L. Schiavi, Applied Catalysis B: Environmental 61 (1–2) (2005) 90–97.
[33] V. Augugliaro, S. Coluccia, V. Loddo, L. Marchese, G. Martra, L. Palmisano, M. Schiavello, Applied Catalysis B: Environmental 20 (1) (1999) 15–27.
[34] M.C. Blount, J.L. Falconer, Applied Catalysis B: Environmental 39 (1) (2002) 39–50.
[35] H. Einaga, S. Futamura, T. Ibusuki, Applied Catalysis B: Environmental 38 (3) (2002) 215–225.
[36] Y. Irokawa, T. Morikawa, K. Aoki, S. Kosaka, T. Ohwaki, Y. Taga, Physical Chemistry Chemical Physics 8 (9) (2006) 1116–1121.
[37] S.A. Larson, J.L. Falconer, Catalysis Letters 44 (1) (1997) 57–65.
[38] M. Lewandowski, D.F. Ollis, Applied Catalysis B: Environmental 43 (4) (2003) 309–327.
[39] L. Cao, Z. Gao, S.L. Suib, T.N. Obee, S.O. Hay, J.D. Freihaut, Journal of Catalysis 196 (2) (2000) 253–261.
[40] G. Martra, S. Coluccia, L. Marchese, V. Augugliaro, V. Loddo, L. Palmisano, M. Schiavello, Catalysis Today 53 (4) (1999) 695–702.
[41] Y. Luo, D.F. Ollis, Journal of Catalysis 163 (1) (1996) 1–11.
[42] R. Mendez-Roman, N. Cardona-Martinez, Catalysis Today 40 (4) (1998) 353–365.
[43] M. Nagao, Y. Suda, Langmuir 5 (1) (1989) 42–47.
[44] M. Fernández-García, A. Fuerte, M.D. Hernández-Alonso, J. Soria, A. Martínez-Arias, Journal of Catalysis 245 (1) (2007) 84–90.
[45] J.M. Coronado, J. Soria, Catalysis Today 123 (1–4) (2007) 37–41.